01

Recombination radiation and compton photoexcitation in the scattering of a photon by an atomic ion

© A.N. Hopersky, A.M. Nadolinsky,¶, R.V. Koneev

Rostov State University for Railway Transportation,
344038 Rostov-on-Don, Russia

¶e-mail: amnrnd@mail.ru

Received December 23, 2022
Revised March 19, 2023
Accepted March 28, 2023.

The analytical structure, absolute values, and angular anisotropy of the doubly differential cross sections of recombination radiation and Compton photoexcitation upon scattering of an X-ray photon by electrons of a multicharged helium-like atomic ion are theoretically predicted.

Keywords: Helium-like ion, recombination radiation, Compton photoexcitation, angular anisotropy, double differential cross section of resonance scattering.

DOI: 10.61011/EOS.2023.04.56364.4482-22

Introduction

A large number of experimental and theoretical works in the fields from plasma physics to cosmology [1–3] are devoted to the study of the effect of recombination radiation, fundamental in the microworld, when a free electron passes into excited and unoccupied states in the core of the discrete spectrum of an atomic ion. In this paper, we study a new mechanism for generating this effect — recombination radiation initiated by inelastic scattering of a photon by the electrons of an atomic ion. Meanwhile, we retain the term „recombination radiation" for the recombination effect (transitions to excited states of the discrete spectrum of an atomic ion) of not a free, but a virtual electron of a continuous spectrum moving in a self-consistent (Hartree-Fock) field of the 1s-vacancy. In this case, the photon absorbed by the atomic ion gives rise to a virtual electron of the continuous spectrum, and the recombination radiation probability amplitude arises as a substructure of the total scattering probability amplitude (Fig. 1, a). In the energy area of the incident and scattered photons under study, we also take into account the Compton photoexcitation effect (Fig. 1, b) — the Landsberg – Mandelstam–Raman effect [4]. Methods for calculating continuum (deceleration emission and nonresonant Compton scattering) structures of total doubly differential cross sections for photon scattering by an atomic ion were developed in a recent paper by the authors [5]. In this paper, as well as in the paper [5], the helium-like ion of the silicon atom (Si^{12+}, nuclear charge of the $Z = 14$ ion; configuration and term of the ground state$[0] = 1s^2[^1S_0]$) is taken as the object of study. Studies of the total doubly differential cross sections for photon scattering by atomic ions are in great demand, in particular, in the interpretation of continuum and resonant structures of X-ray emission spectra from hot astrophysical objects (for example, see [6,7]).

Method theory

Let us consider the processes of resonant (transitions to the final states of the discrete spectrum) inelastic scattering of a photon by electrons of a helium-like atomic ion:

$$\omega + [0] \to 1sxp(^1P_1) \to \begin{Bmatrix} K_s \\ K_d \end{Bmatrix} + \omega_C, \qquad (1)$$

$$K_s = 1sns(^1S_0), \qquad K_d = 1smd(^1D_2), \qquad (2)$$

$$\omega + [0] \to 1snl(^1L_J) + \omega_C. \qquad (3)$$

In (1), (3) and further, the atomic system of units ($e = \hbar = m_e = 1$), $n \geq 2$, $m \geq 3$, $l \geq 0$, $J = L$, $\omega(\omega_C)$ — energy of the incident (scattered) photon and$x$ — energy of the electron of the continuous spectrum of the intermediate (virtual) scattering state, $x \in [0 : \infty)$. Scattering through

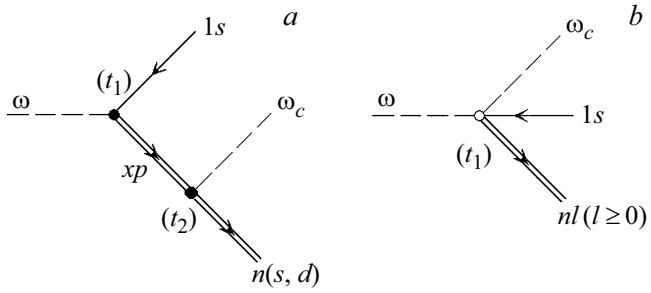

Figure 1. Probability amplitudes of resonant inelastic photon scattering by a helium-like atomic ion (Si^{12+}) in the representation of Feynman diagrams: (a) recombination radiation; (b) Compton photoexcitation. Right arrow — electron, left arrow — vacancy. Double line — the state was obtained in the Hartree-Fock field of the1s-vacancy. The black (light) circle — the interaction vertex along the operator of the radiative (contact) transition. $\omega(\omega_C)$ — incident (scattered) photon. Time direction — left to right ($t_1 < t_2$).

channels (2) corresponds to an initiated recombination radiation (Fig. 1, *a*) according to the radiative transition operator:

$$\hat{R} = -\frac{1}{c}\sum_{n=1}^{N}\left(\hat{p}_n\hat{A}_n\right). \quad (4)$$

Scattering along channel (3) corresponds to Compton photoexcitation (Fig. 1, *b*) according to the contact interaction operator:

$$\hat{Q} = \frac{1}{2c^2}\sum_{n=1}^{N}\left(\hat{A}_n\hat{A}_n\right). \quad (5)$$

B (4) and (5) are determined: $\hat{A}_n$ — the operator of the electromagnetic field in the representation of the second quantization, $\hat{p}_n$ — the momentum operator of the n- ion electron,c — the speed of light in vacuum and N — the number of electrons in the ion.

When constructing the scattering probability amplitudes, the second order (in terms of the fine structure constant) of the quantum-mechanical perturbation theory is taken. Analytical structures of doubly differential scattering cross sections are established by methods of the algebra of photon creation (destruction) operators, the theory of irreducible tensor operators, and the theory of non-orthogonal orbitals [8]. For the recombination radiation cross section (RR; Fig. 1, *a*, 2, *a*) in the dipole approximation for the $\hat{R}$-operator [5] we obtain:

$$\frac{d^2\sigma_{RR}}{d\omega_C d\Omega_C} \equiv \sigma_{RR}^{(2)} = r_0^2\frac{\omega_C}{\omega}\eta\mu\sum_{n=2}^{\infty}a_{ns}G_{ns}, \quad (6)$$

$$a_{ns} = \frac{1}{\in_0}\left(\frac{\omega_{ns}}{\omega}\langle 1s_0|\hat{r}|\varepsilon p_+\rangle\langle\varepsilon p_+|\hat{r}|ns_+\rangle\right)^2, \quad (7)$$

$$G_{ns} = \frac{1}{\gamma_b\sqrt{\pi}}\exp\left\{-\left(\frac{\omega_{ns}-\omega_C}{\gamma_b}\right)^2\right\}, \quad (8)$$

where Ω_C — spatial angle of emission of the scattered photon, r_0 — classical electron radius, $\eta = (2/9)\pi^2\omega^4\langle 1s_0|1s_+\rangle^2$, $\eta_0 = 27.21$, $\varepsilon = \omega - I_{1s}$, $\omega_{ns} = \omega - I_{1sns}$, I_{1s} — ionization threshold energy $1s^2$-ion shell, I_{sns} — energy of $1s \to ns$-transition, $\gamma = \Gamma_{beam}/(2\sqrt{\ln 2})$ and Γ_{beam} — the width of the spectral resolution of the proposed experiment. The Gauss-Laplace spectral function appears in the Fermi „golden rule“ when the$\delta(\omega_{ns} - \omega_C)$ — Dirac function is replaced by G_{ns}. In (7) the length form for the one-electron radiative transition operator is realized. A potential discrepancy between the forms of length and velocity in the single-configuration Hartree–Fock approximation can be removed by passing, for example, to the multiconfiguration Hartree–Fock approximation when constructing the complete wave functions of the scattering states. The indices „0“ and „+“ correspond to the radial parts of the electron wave functions obtained by solving the self-consistent Hartree-Fock field equations for the configurations of the main ([0]), intermediate ($[1s_+xp_+]$), and final ($[1s_+nl_+]$) ion states. As expected, the section (6) satisfies the asymptotic condition for the disappearance of resonances of the recombination radiation: at $\omega \to \infty$ $\sigma_{RR}^{(2)} \sim 1/(\gamma_b\omega^3) \to 0$ for $\gamma_b > 0$. In section (6), the contribution of the K_d scattering channel was not taken into account, since, as the calculation showed, it is four (or more) orders of magnitude less than the contribution of the K_s- scattering channel. For the polarization vectors of the incident ($\mathbf{e}$) and scattered ($\mathbf{e}_C$) photons, the axisymmetric (with respect to $\mathbf{k}$ — wave vector of the incident photon) parameter $\mu = (\mathbf{e}\cdot\mathbf{e}_C)^2$ in (6) determines the effect of angular anisotropy recombination cross section. It is specified in accordance with the three schemes of the proposed experiment. The first scheme — photon polarization vectors are perpendicular ($\perp$) to the scattering plane. The second scheme — photon polarization vectors are parallel ($\parallel$) to the scattering plane. The third scheme — scheme with unpolarized (UP) photons. The scattering plane passes through the wave vectors of the incident and scattered ($\mathbf{k}_C$) photons. As a result, we obtain:

$$\mu^{\perp} = 1, \quad (9)$$

$$\mu^{\parallel} = \cos^2\theta, \quad (10)$$

$$\mu_{NP} = \frac{1}{2}(\mu^{\perp} + \mu^{\parallel}), \quad (11)$$

where θ — scattering angle (angle between the vectors $\mathbf{k}$ and $\mathbf{k}_C$). For the Compton photoexcitation cross section (CPh; Fig. 1, *b*, 2, *b*) outside the framework of the dipole approximation for the $\hat{Q}$ operator, we obtain:

$$\sigma_{CPh}^{(2)} = r_0^2\frac{\omega_C}{\omega}\mu\sum_{n=2}^{\infty}b_{np}G_{np}, \quad (12)$$

$$b_{np} = \frac{6}{\in_0}\left(\langle 1s_0|1s_+\rangle\left\langle 1s_0\left|\hat{j}_1(qr)\right|np_+\right\rangle\right)^2, \quad (13)$$

where $\hat{j}_1$ — spherical Bessel function of the first kind of the first order and $q = |\mathbf{k} - \mathbf{k}_C|$. Note that in the dipole approximation for $\hat{Q}$ — the operator $\hat{j}_1 \to 0$ and $\sigma_{CPh}^{(2)} \to 0$. In the (12) cross section, the contribution of the photoexcitation states with $l \neq 1$ was not taken into account, since, as the calculation showed, it is three (or more) orders of magnitude smaller than the contribution of the $1snp$ photoexcitation states. As a result, the quantum interference of the probability amplitudes of the scattering channels (1) and (3) is practically absent. The asymptotic condition for the disappearance of the resonances of the Compton photoexcitation takes the following form: at $\omega \to \infty$ $\sigma_{CPh}^{(2)} \sim 1/(\gamma_b\omega^{7/2}) \to 0$ for $\gamma_b > 0$.

Results and Discussion

The calculation results as part of our theory are presented in Fig. 2, 3 and in the table. The value of the ionization threshold energy $1s^2$-shell of the ion Si^{+12} $I_{1s} = 2437.659$ eV is taken from [9]. The transition energies

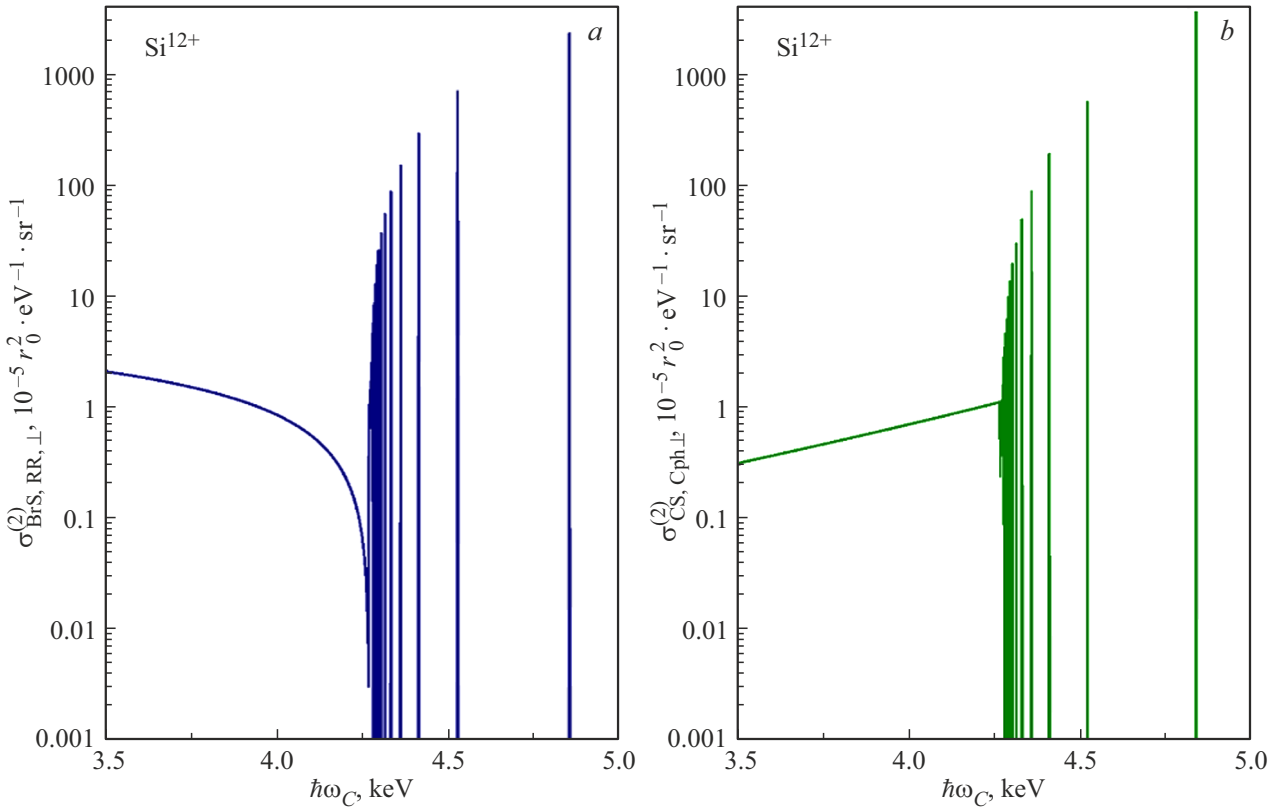

Figure 2. Double differential cross sections for inelastic photon scattering by the Si^{12+} ion for $\perp$ scheme of the experiment: (a) bremsstrahlung cross-section (BrS) and recombination radiation (RR), (b) cross nonresonant Compton scattering (CS) and Compton photoexcitation (CPh). Incident photon energy $\hbar\omega = 6.7$ keV, $\hbar\omega_C$ — scattered photon energy. Angle of scattering$\theta = 90°$. Width of the spectral resolution of the experiment $\Gamma_{beam} = 0.5$ eV.

for I_{1snS} $n \in [2; 7, 8, 9, 10]$ and I_{1snp} for $n \in [2; 10]$ are taken from [10]. The I_{1sns} values for $n \in [3; 6]$ are taken from [11]. For $n \in [11; \infty]$, the transition energies are obtained by an approximation of the form

$$I_{1snl} = I_{1s} - \frac{1}{n^2}\left(\alpha + \frac{1}{n}\beta\right), \qquad (14)$$

where the numbers α and β are determined by the values I_{1sml} for $m = 9, 10$. The probability amplitudes of the dipole $J_{ns} = \langle \varepsilon p_+ | \hat{r} | ns_+ \rangle$ and contact $J_{np} = \langle 1s_0 | \hat{j}_1(qr) | np_+ \rangle$ transitions for $n \in [2; 10]$ were obtained on the radial parts of the wave functions of the Hartree $-$Fock approximation at an incident photon energy $\omega = 6700$ eV (energy K_α- emission line Fe^{24+} [12]) and angle of scattering $\theta = 90°$ (Fig. 2). For $n \in [11; \infty)$ integrals J_{ns} and J_{np} are obtained by approximation of the form

$$J_{nl} = \frac{1}{n^2}\left(\varsigma + \frac{1}{n}\rho + \frac{1}{n^2}\chi\right), \qquad (15)$$

where the numbers ς, ρ and χ are determined by the values J_{ml} for $m = 8, 9, 10$. When constructing the indicatrix of the Compton photoexcitation $1s \to 2p$ in the probability amplitude J_{2p}, the dependence $\hat{j}_1$ of the Bessel function on the angle of scattering [see (17) and Fig. 3, b] is taken into account. The results in Fig. 2 and in the table at $\omega_C > \omega - I_{1s}$ demonstrate pronounced resonant structures of the spectra of recombination radiation (Fig. 2, a) and Compton photoexcitation (Fig. 2, b). Continuum structures of total doubly differential scattering cross sections for $\omega_C \le \omega - I_{1s}$ (bremsstrahlung (BrS, Fig. 2, a) and nonresonant Compton scattering (CS, Fig. 2, b /)) are taken from the paper of the authors [5]. The theoretical width of the two-photon decay $\Gamma_{1s2s} \cong 6.2 \cdot 10^{-8}$ eV of the metastable state $1s2s(^1S_0)$ was obtained by approximating

Spectral data of the leading resonances of the recombination radiation and ($xp \to ns$)Compton photoexcitation ($1s \to np$) in $\perp$ — scheme of the experiment: $\hbar\omega_C$ — scattered photon energy, incident photon energy $\hbar\omega = 6.7$ keV, experimental spectral resolution width $\Gamma_{beam} = 0.5$ eV, angle of scattering $\theta = 90°$

nl	$\hbar\omega_C$, eV	$\sigma^2, 10^{-2} \cdot r_0^2$ eV^{-1}sr^{-1}
2s	4845.35	2.290
3s	4520.55	0.685
4s	4407.31	0.289
2p	4835.01	3.546
3p	4517.44	0.548
4p	4405.94	0.187

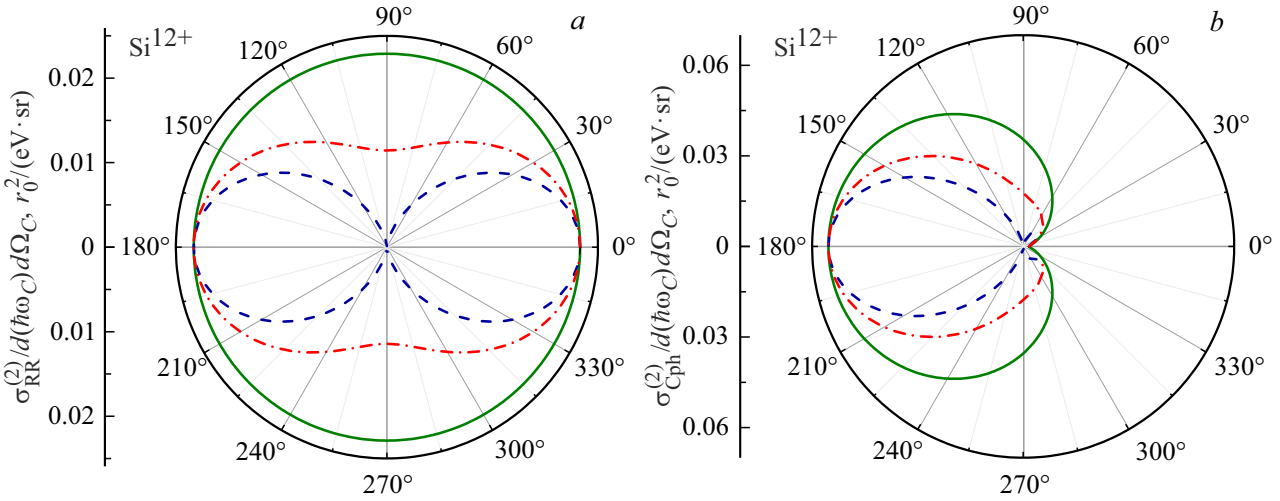

Figure 3. Indicatrices (a) of recombination radiation and (b) of Compton photoexcitation for the Si^{12+} ion with polar radius and polar angle at fixed energies of the incident ($\hbar\omega = 6.7\,\text{keV}$) and scattered $\hbar\omega = 4.845\,\text{keV}$ ($xp \to 2s,\ RR$), $\hbar\omega_C = 4.835\,\text{keV}$ ($1s \to 2p,\ CPh$)) photons. Width of the spectral resolution of the experiment $\Gamma_{\text{beam}} = 0.5\,\text{eV}$. Scheme of the experiment: $\perp$ (solid curve), $\parallel$ (dashed curve), unpolarized photons (dash-dotted curve).

the results of [13] ($He-Ne^{8+}$). The theoretical width of the dipole-allowed decay of the $1s2p(^1P_1)\Gamma_{1s2p} \cong 3 \cdot 10^{-2}\,\text{eV}$ state was obtained by interpolating the results of [14] (Na^{9+}), [15] (Ar^{16+}) and [16] (Cr^{22+}). The obtained values for the resonance widths of the recombination radiation ($\Gamma_{1sns} \cong \Gamma_{1s2s}$) are inaccessible to modern experiment, including telescopes in astrophysics [17]. However, the schemes of the proposed experiment outlined above can be implemented, in particular, by combining methods for generating multiply charged ions and trapping them in a „trap“ with subsequent scattering of X-ray free-electron laser radiation (XFEL) [18]. Therefore, as the width of the spectral resolution of the experiment for all states, we took the value $\Gamma_{beam} = 0.5\,\text{eV}$, achieved in a series of XFEL experiments [19,20]. In this case, in formulas (6) and (12) the summation is limited by the value of the principal quantum number $n_{\max} = 500$. The results in the table give an idea of the magnitude orders of the leading resonances of the scattering cross sections for the accepted value of Γ_{beam}. The transition to the theoretical values $\gamma_{1sn(s,p)}$ reveals the fact that the resonances of the Compton photoexcitation are practically suppressed in comparison with the resonances of the recombination radiation in any energy range of the photon incident on the ion:

$$\sigma^{(2)}_{1snp}/\sigma^{(2)}_{1sns} \sim \Gamma_{1sns}/\Gamma_{1snp} \sim 10^{-6}. \qquad (16)$$

The results in Fig. 3, a qualitatively reproduce those for the bremsstrahlung of paper [5]. The quantitative difference (the scattering cross section goes to zero at $\theta = 90°$ in the $\parallel$-scheme of the experiment) from the results [5] is due to the fact that in (6) the contribution of the $K_d$scattering channel is discarded, negligible compared to the contribution of the K_s scattering channel. In case of bremsstrahlung [5] K_s- and K_d-scattering channels make comparable contributions to the scattering cross section at $\theta = 90°$ in the $\parallel$-scheme of the experiment. The results in Fig. 3, b demonstrate a strong asymmetry with respect to the angles $\theta = 0°$ and $\theta = 180°$ of the scattering indicatrix for Compton photoexcitation resonances. The reason for the asymmetry lies in the analytical structure of the q parameter of the j_1 Bessel function:

$$q \sim \left(\omega^2 + \omega_C^2 - 2\omega\omega_C \cos\theta\right)^{1/2}. \qquad (17)$$

According to (17), $q \sim \omega - \omega_C$ at $\theta \to 0°$, while $q \sim \omega + \omega_C$ at $\theta \to 180°$. As a result, for all schemes of the proposed experiment

$$J^2_{2p}(\theta = 0°) \ll J^2_{2p}(\theta = 180°). \qquad (18)$$

Thus, during „forward“ scattering, a scattering cone arises with an opening angle $2\theta \cong 50°$, in which the resonances of the Compton photoexcitation (Fig. 3, b) are practically suppressed in comparison with the resonances of the recombination radiation (Fig. 3, a).

Conclusion

The total doubly differential cross section of inelastic X-ray photon scattering by electrons of a multiply charged helium-like atomic ion is theoretically studied. The structures of the spectra of initiated recombination radiation and Compton photoexcitation and their angular anisotropy are established. In this case, the angular anisotropy of the Compton photoexcitation is accompanied by a strong asymmetry of the scattering phase functions. It is shown that, when passing to the theoretical values of the spectral decay widths of the metastable ($1sns$) and dipole-allowed ($1snp$) final scattering states, the resonances

of the Compton photoexcitation are practically suppressed in comparison with the resonances of the recombination radiation. The results obtained are predictive.

Conflict of interest

The authors declare that they have no conflict of interest.

References

[1] B. Zhu, A. Gumberidze, T. Over, G. Weber, Z. Andelkovic, A. Bräuning–Demian, R.J. Chen, D. Dmytriev, O. Forstner, C. Hahn, F. Herfurh, M.O. Herdrich, A.–M. Hillenbrand, A. Kalinin, Ph. Pfafflein, M.S. Sanjari, R.S. Sidhu, U. Spillmann, R. Schuch, S. Schippers, S. Trotsenko, L. Varga, G. Vorobyev, Th. Stöhlker. Phys. Rev. A, **105** (5), 2804 (2022). DOI: 10.1103/PhysRevA.105.052804

[2] L. Hart, J. Chluba. Mon. Not. R. Astron. Soc., **519** (3), 3664 (2023). DOI: 10.1093/mnras/stac 3697

[3] R.A. Sunyaev, J. Chluba. Astron. Nachr. AN, **330**, 657 (2009). DOI:10.48550/arXiv.0908.0435

[4] A.N. Hopersky, A.M. Nadolinsky, V.A. Yavna. ZhETF, **130** (4), 579 (2006). (in Russian) DOI: 10.7868/S0370274X17140090

[5] A.N. Hopersky, A.M. Nadolinsky. Pis'ma v ZhETF, **115** (8), 469 (2022) (in Russian). DOI: 10.31857/S1234567822080110

[6] A.W. Shaw, J.M. Miller, V. Grinberg, D.J.K. Buisson, C.O. Heinke, R.M. Plotkin, J.A. Tomsick, A. Bahramian, P. Gandhi, G.R. Sivakoff. Mon. Not. R. Astron. Soc., **516** (1), 124 (2022). DOI: 10.1093/mnras/stac2213

[7] P. Chakraborty, G. J. Ferland, M. Chatzikos, A. C. Fabian, S. Bianchi, F. Guzmán, Y.Su. Astrophys. J., **935** (2), 70 (2022). DOI: 10.3847/1538-4357/ac7eb9

[8] A.N. Hopersky, A.M. Nadolinsky, S.A. Novikov. Phys. Rev. A, **98** (6), 3424 (2018). DOI: 10.1103/PhysRevA.98.063424

[9] V.A. Yerokhin, V. Patkóš, K. Pachucki. Phys. Rev. A, **106** (2), 2815 (2022). DOI: 10.1103/PhysRevA.106.022815

[10] W. C. Martin, R. Zalubas. J. Phys. Chem. Ref. Data, **12** (2), 323 (1983).

[11] V. A. Yerokhin,A. Surzhykov. J. Phys. Chem. Ref. Data, **48** (3), 3104 (2019). DOI: 10.1063/1.5121413

[12] V. Malyshev, Y.S. Kozhedub, D.A. Glazov, I.I. Tupitsyn, V.M. Shabaev. Phys. Rev. A, **99** (1), 501(R) (2019). DOI: 10.1103/PhysRevA.99.010501

[13] G.W.F. Drake, G.A. Victor, A. Dalgarno. Phys. Rev., **180**, 25 (1969). DOI: 10.1103/PhysRev.180.25

[14] J.E. Sansonetti. J. Phys. Chem. Ref. Data, **37** (4), 1659 (2008). DOI: 10.1063/1.2943652

[15] J. Machado, C.I. Szabo, J.P. Santos, P. Amaro, M. Guerra, A. Gumberidze, G. Bian, J.M. Isac, P. Indelicato. Phys. Rev. A, **97** (3), 2517 (2018). DOI: 10.1103/PhysRevA.97.032517

[16] T. Shirai, Y. Nakai, T. Nakagaki, J. Sugar, W.L. Wiese. J. Phys. Chem. Ref. Data, **22** (5), 1279 (1993).

[17] S.R. Bandler, J.A. Chervenak, A.M. Datesman, A.M. Devasia, M.J. DiPirro, K. Sakai, S.J. Smith, T.R. Stevenson, W. Yoon, D. Bennett, B. Mates, D. Swetz, J.N. Ullom, K.D. Irwin, M.E. Eckart, E. Figueroa-Feliciano, D. McCammon, K. Ryu, J. Olson, B. Zeiger. J. Astron. Telesc. Instrum. Syst., **5** (2), 1017 (2019). DOI: 10.1117/1.JATIS.5.2.021017

[18] P. Indelicato. J. Phys. B, **52** (23), 2001 (2019). DOI: 10.1088/1361-6455/ab42c9

[19] D. Zhu, M. Cammarata, J.M. Feldkamp, D.M. Fritz, J.B. Hastings, S. Lee, H.T. Lemke, A. Robert, J.L. Turner, Y. Feng. Appl. Phys. Lett., **101** (3) 4103 (2012). DOI: 10.1063/1.4736725

[20] N. Kujala, W. Freund, J. Liu, A. Koch, T. Falk, M. Planas, F. Dietrich, J. Laksman, T. Maltezopoulos, J. Risch, F. Dall'Antonia, J. Grünert. Rev. Sci. Instrum., **91** (10) 3101 (2020). DOI: 10.1063/5.0019935

Translated by E.Potapova